ASCE/SEI 41 Assessment of Reinforced Concrete Buildings: Benchmarking Linear Procedures and FEMA P-2018 with Empirical Damage Observations

Andrew Sen,[a)] M.EERI, Dustin Cook,[b)] M.EERI, Abbie Liel,[c)] M.EERI, Tarbin Basnet,[d)] Ariel Creagh,[e)] Hamid Khodadadi Koodiani,[d)] Russell Berkowitz,[f)] M.EERI, Wassim Ghannoum,[d)] M.EERI, Ayse Hortacsu,[g)] M.EERI, Insung Kim,[e)] M.EERI, Dawn Lehman,[g)] Laura Lowes,[h)] M.EERI, Adolfo Matamoros,[d)] M.EERI, Farzad Naeim,[h)] M.EERI, Siamak Sattar,[b)] M.EERI, and Rob Smith[j)]

ABSTRACT

The U.S. consensus standard for seismic evaluation and retrofit of existing buildings, ASCE/SEI 41, establishes provisions for seismic analysis procedures that vary in complexity and fidelity. Although ASCE/SEI 41 provides detailed nonlinear dynamic procedures, most engineers rely on simpler methods to evaluate building seismic performance and retrofit, particularly the ASCE/SEI 41 linear procedures and, more recently, the FEMA P-2018 methodology for evaluating collapse potential. Under ideal conditions, these procedures identify similar structural deficiencies. However, evaluation outcomes in practice may differ due to the complexity of real building response, approximations used in modeling and analysis, and level of intentional conservativism that reflects the limitations of the procedures. To quantify these differences, this study considers six reinforced concrete buildings that sustained damage in real earthquakes or in shake table tests and compares the performance assessed by the ASCE/SEI 41 linear and nonlinear dynamic procedures, as well as the FEMA P-2018 seismic evaluation methodology.

[a)] Marquette University, Milwaukee, WI 53201
[b)] National Institute of Standards and Technology, Gaithersburg, MD 20899
[c)] University of Colorado, Boulder, CO 80309
[d)] University of Texas, San Antonio, TX 78249
[e)] Degenkolb Engineers, San Francisco, CA 94105
[f)] Forell | Elsesser Engineers, San Francisco, CA 94111
[g)] Applied Technology Council, Redwood City, CA 94065
[g)] University of Washington, Seattle, WA 98195
[h)] Farzad Naeim, Inc., Irvine, CA, 92618
[j)] COWI, Oakland, CA 94607

The results show that, for these highly damaged buildings, the overall performance level estimated from the ASCE/SEI 41 linear procedures is consistent with observed damage. In general, the procedures also correctly identify the story with the most damage and the component failure mode. However, the ASCE/SEI 41 linear procedure generally underpredicts drift response and greatly overpredicts peak floor accelerations. Though these are not directly used to evaluate structural performance, they are related to component deformation and force demands, respectively. Moreover, the linear procedures predict damage in components that would be precluded by yielding or failure of other components in the load path. Results from the FEMA P-2018 methodology for the six buildings provide more distinction between buildings than the ASCE/SEI 41 Collapse Prevention performance level. The results also suggest the FEMA P-2018 limit-state mechanism analysis can provide supplemental information to support and improve the ASCE/SEI 41 linear procedures.

INTRODUCTION

Seismic performance evaluation is an important tool employed to identify vulnerabilities in the structural components of existing buildings, and, ultimately, inform decisions on future building use and retrofit design. These decisions may have long-term effects on the community, including population displacement in the aftermath of an earthquake event and the life-cycle carbon emissions related to extensive repair or replacement of a building. While many such methodologies have been developed, the ASCE/SEI 41 Seismic Evaluation and Retrofit of Existing Buildings document standardizes these evaluations for U.S. practice (ASCE 2017) and has been adopted formally in many jurisdictions and by the General Services Administration for seismic design of federal facilities. The ASCE/SEI 41 provisions for systematic evaluation and retrofit (i.e., Tier 3 evaluation) define modeling guidelines and performance-based acceptance criteria for seismic structural analysis. Tier 3 evaluations are the most involved of those presented in ASCE/SEI 41 and can be conducted with either linear or nonlinear modeling and either static or dynamic representations of seismic loading. Performance is evaluated on a component-action basis by comparing simulated demand to acceptance criteria limits; building performance is dictated by the worst performing component. These limits are dependent on the structural component and system, and based on

existing test data (e.g., Elwood et al. 2007; Elwood and Eberhard 2009; Ghannoum and Matamoros 2014; ACI 2017)

In this study, we compare the outcomes of the linear procedures in ASCE/SEI 41 and the new mechanism-based Seismic Evaluation of Older Concrete Buildings for Collapse Potential (FEMA 2018), FEMA P-2018, to the observed damage sustained by four real reinforced concrete (RC) buildings damaged in earthquakes and two RC building experimental specimens tested on shake tables. Both the ASCE/SEI 41 and FEMA P-2018 procedures quantify seismic performance, but FEMA P-2018 was developed as a screening tool that, for example, could be used to identify evaluation or retrofit priorities within a building inventory with a lower level of effort than an ASCE/SEI 41 Tier 3 evaluation. As such, we do not evaluate FEMA P-2018 as an outright replacement for Tier 3 evaluations in ASCE/SEI 41, but we explore its implications in the context of the other evaluation methods. We focus on RC buildings because they are high priorities for seismic evaluation and retrofit in many earthquake-prone jurisdictions due to their known seismic vulnerabilities. The set of buildings comprises both frame and wall structures and is selected for assessment based on the availability of: (1) building drawings providing the information needed to create structural analysis models, (2) documentation of earthquake damage (e.g., photos, reports, and–in some cases–detailed field or experimental instrumentation), and (3) documentation of ground motion(s) at or near the site. In addition, we focus on buildings located in the U.S. or representative of typical U.S. construction and avoided buildings that had unique or irregular features such as low construction quality, widespread use of masonry, or significant eccentricities in geometry (with the exception of one building, noted below). Detailed descriptions of the buildings and damage observations are provided in the companion paper (Cook et al. 2023) and NIST GCR 22-917-50 (NIST 2022). Cook et al. (2023) also compared the observed damage in these buildings to assessments following the ASCE/SEI 41-17 Nonlinear Dynamic Procedure (NDP) using recorded ground motions for each building. This comparison reveals that: (1) the NDP procedure is generally able to identify the story mechanism, peak drift demands at the critical story, components with the most severe damage, and component failure mode(s); (2) there are larger discrepancies between measured and simulated drifts at noncritical locations and between measured and simulated floor accelerations; and (3) for some buildings, the NDP overestimates the extent of damage.

In this paper, we compare the seismic performance evaluation outcomes for the same buildings using (1) static, response-spectrum, and response-history analysis using the ASCE/SEI 41-17 Linear Static Procedure (LSP) and Linear Dynamic Procedure (LDP) and (2) the FEMA P-2018 collapse-based Building Rating. The results are benchmarked against the observed damage and ASCE/SEI 41 NDP evaluation outcomes. For each evaluation methodology, we compare the predicted outcomes (e.g., distribution and severity of simulated responses and damage) to the observed damage and "state-of-the-art" practice using the ASCE/SEI 41-17 NDP. Table 1 describes the six buildings, the evaluation methodologies, and structural analysis software we use to assess each. Due to practical limitations, the number and type of evaluation methodologies studied for each building vary. The goals of this paper are to (1) benchmark the ASCE/SEI 41-17 linear assessment procedures against earthquake observations and other methods, (2) assess how well the linear procedures match real building performance, and (3) identify what significant improvements nonlinear or mechanism-based procedures such as FEMA P-2018 provide.

Table 1. Buildings and evaluation methodologies

Building or Specimen	Brief Description	ASCE/SEI 41 Linear Procedures				ASCE/SEI 41 NDP	FEMA P-2018
		Static	Response Spectrum	Response History	Software	Software	
UC Berkeley test frame	Experimental test; 2D, 3-story RC frame	●	●	●	ETABS[b]	Perform-3D[c]	●
E-Defense test	Experimental test; 4-story RC frame and wall		●	●	ETABS	OpenSees[d], Perform3D	●
Pyne Gould[a]	Real building, not instrumented; 5-story RC wall		●	●	ETABS	OpenSees	●
Imperial County Services	Real building, instrumented; 6-story RC frame and wall			●	OpenSees	OpenSees	
Van Nuys Hotel	Real building, instrumented; 7-story RC frame with limited masonry infill		●	●	ETABS	OpenSees	
Nanhua District Office	Real building, not instrumented; 3-story RC frame with masonry infill			●	SAP2000[e]	OpenSees	●

Note: Empty cells indicate evaluation methodology is not studied.
[a]Not compliant with linear procedure due to torsional strength irregularity but evaluated for engineering interest.
[b]CSI (2020a), https://www.csiamerica.com/products/etabs/
[c]Perform3D (2020), "Performance based design of 3D structures" Computers and Structures Inc., https://www.csiamerica.com/products/perform3d
[d]McKenna et al. (2000), https://opensees.berkeley.edu/
[e]CSI (2020b), https://www.csiamerica.com/products/sap2000/

ASCE/SEI 41 LINEAR PROCEDURES

Among Tier 3 evaluations following ASCE/SEI 41, procedures based on linear structural analysis are the most frequently used in practice due to their relative speed, simplicity, and accessibility (e.g., SEAOSC [2017]). Although the material response is linear-elastic, these procedures incorporate adjustments to building deformations and acceptance criteria to account for "probable nonlinear response" (ASCE/SEI 2017, Section C7.3). As with the ASCE/SEI 41 NDP, the structural analysis performed can be static or dynamic; for linear procedures, dynamic analysis refers to both response-spectrum and response-history analysis. To assess the outcomes from the ASCE/SEI 41 linear procedures in this section, we directly compare the simulated component damage states and system damage mechanisms to the observed damage and corresponding NDP results for the buildings in Table 1. Unless otherwise indicated, the results in this section are for the response-history analysis; the Linear Static Procedure (LSP) was also employed for one building.

With all ASCE/SEI 41 linear procedures, the predicted performance is generally intended to be more conservative than that of nonlinear procedures, since linear models do not simulate strength and stiffness degradation due to spalling, yielding, fracture, and other damage mechanisms. Indeed, previous studies have indicated that the linear procedures are more conservative for modern steel and concrete moment frames (Sattar 2018; Harris and Speicher 2018; Sattar and Hulsey 2015), due in part to conservatism in acceptance criteria and linear assessments' overestimation of demands in deformation-controlled elements that are protected by yielding or failure of other components. However, other studies have suggested they may be less conservative than nonlinear procedures for modern steel braced frames (Speicher and Harris 2016a; Speicher and Harris 2016b; Speicher and Harris 2018) because of the concentration of damage in the nonlinear assessment that is not identified in linear assessment. A key focus in this study is to benchmark the level of conservatism of the linear procedures against measured or observed building performance.

METHODS

To assess the outcomes from the ASCE/SEI 41-17 Linear Dynamic Procedures (LDP), we develop linear simulation models of the six buildings identified in Table 1 and subject each model to the best-estimate ground motions representing the expected shaking during the earthquake or experiment, as previously reported (Cook et al. 2023). In these simulation

models, all components are modeled with linear-elastic properties. The corresponding internal forces and system displacements are determined using the procedures described per ASCE/SEI 41-17 Sections 7.4.1 and 7.4.2 and compared against the acceptance criteria of ASCE/SEI 41-17 Section 7.5.2.2 for deformation- and force-controlled actions. The magnitude and distribution of inelastic demands are defined in terms of demand-capacity ratios (DCRs) (ASCE 41-17 Eq. 7-16 and 7-36). For deformation-controlled actions, these DCRs include the component modification factor (*m*-factor), which accounts for expected ductility capacity (Eq. 1).

$$DCR = \frac{Q_{UD}}{m\kappa Q_{CE}} \tag{1}$$

In Eq. 1, Q_{UD} is the force (or deformation-controlled action) caused by gravity loads and earthquake forces and Q_{CE} is the expected strength (capacity) of a component's deformation-controlled action (ASCE/SEI, 2017). The *m*-factors are associated with the action of interest at the selected structural performance levels of Immediate Occupancy (IO), Life Safety (LS), or Collapse Prevention (CP) (ASCE/SEI 41-17, Eq. 7-36). The components evaluated here are considered primary components with the exception of the framing members in the Pyne Gould building, which were designed to resist gravity loads only, have low strength and stiffness, and are thus classified as secondary components. Primary component *m*-factors for LS and CP performance levels are generally calibrated from capping deformation data, whereas the corresponding nonlinear acceptance criteria are based on failure deformation (see ASCE/SEI 41-17 Section 7.6.3); this is a source of intentional conservatism in the linear procedures since strength degradation is not simulated in linear analysis. As described in Table 2 for RC columns, these performance levels are defined to align with key physical descriptors of component damage expected to be observed in buildings at each performance level. In application of ASCE/SEI 41, individual component performance defines building performance, but it is recognized that performance of real buildings is complex and, in a sense, based on aggregate component performance; hence, engineering judgment is required to correlate observed damage to ASCE/SEI 41 performance levels. To avoid additional conservatism when comparing with observed damage, we take the knowledge factor, κ, as 1.0.

We determine the ASCE/SEI 41 assessment of overall building performance from the *DCRs* of all components within the building; if any component *DCR* is greater than 1.0 for a given Performance Level the building fails to meet the acceptance criteria. In most of the

results, for deformation-controlled actions, we report *DCRs* divided by the *m*-factor for CP, where a *DCR* exceeding 1.0 indicates a component that fails the CP Performance Level and a *DCR* less than 1.0 indicates that the component passes CP. The *m*-factors associated with the CP acceptance criteria are taken from Tables 10-10, 10-13, 10-14,10-16, 10-21, and 10-22 in ASCE/SEI 41-17. These values are calculated separately for each action (e.g., column flexure, shear and axial *DCR*). Some of these actions are deformation controlled (e.g., flexure and shear), and some are force controlled (e.g., axial).

Table 2. Nonductile column damage patterns associated with each structural performance level, based on RC columns described in Table C2-4 and Section C10.4.2.2.2 of ASCE/SEI 41-17 (ASCE 2017)

ASCE/SEI 41 Performance States	Description
Immediate Occupancy (IO)	Minor cracking, limited yielding, and minor spalling of concrete cover
Life Safety (LS)	Spalling of cover and shear cracking in ductile columns; minor spalling in nonductile columns
Collapse Prevention (CP)	Extensive cracking and hinge formation in ductile columns; limited cracking or splice failure in nonductile columns

MODELING APPROACHES

All simulation models are three dimensional, except for the model of the two-dimensional UC Berkeley test frame. These three-dimensional models are intended to reflect the system-level torsional and component-level biaxial load effects present in the real structures. We defined beams and columns with line elements and walls as either shell elements (Pyne Gould, E-Defense test) or line elements with a rigid "beam" at the top to represent wall length (Imperial County Services). Component effective stiffnesses are defined to account for the reduced effective stiffness, as defined in Table 10-5 of ASCE/SEI 41-17. For flexural rigidity of walls, these values are $0.35E_{cE}I_{g,}$ where E_{cE} is the modulus of elasticity of concrete determined with expected material properties and I_g is the moment of inertia of gross concrete section, neglecting reinforcement. Column flexural stiffness is $0.3E_{cE}I_g$ for columns with relatively light axial loads (and varies for the other cases). Beam flexural stiffness is 0.3-$0.4E_{cE}I_g$ in Table 10-5; but, where appropriate, we modify I_g to account for the stiffness effect of a monolithic slab. For the UC Berkeley test frame, joints are modeled directly with a panel-zone element, while the E-Defense Test, Imperial County Services, and Nanhua District Office models use rigid offsets to represent joints implicitly depending on the relative strengths of beams and columns framing into the joints (ASCE 41-17, Section 10.4.2.2). For Pyne Gould, Van Nuys Hotel, and Nanhua District Office, slabs are modeled as shell elements; for the E-Defense test and Imperial County Services, slabs are modeled using a rigid diaphragm

consistent with ASCE/SEI 41-17 Section 7.2.9. Additional details about the general modeling approach are provided in Cook et al. (2023).

ASCE/SEI 41-17 Section 10.6.2 requires consideration of both full- and partial-height masonry infill. Both the Van Nuys Hotel and the Nanhua District Office buildings had masonry infill walls in some locations. In the Van Nuys Hotel building, there was a 1-inch gap around the infill panels, however, due to the observed damage, the panels are thought to have affected seismic performance, and therefore are included in the model. The Nanhua District Office had both partial-height and full-height masonry infill. For both buildings, the masonry infill was modeled with diagonal struts, as indicated by ASCE/SEI 41-17. Alternative masonry infill modeling approaches using shell elements or rigid offsets (to represent shortened column height due to the effects of partial-height infill) result in similar outcomes in the Nanhua District Office model; when masonry infill is not modeled, the evaluation outcomes are inconsistent with observed damage, as expected. While we included masonry infill walls in the models to capture the effects on the overall building behavior and better estimate the demands placed on the RC components, we do not evaluate the acceptance criteria for the infill walls due to our focus on the RC components and systems.

We apply gravity loads, including the dead load and 25% of the assumed design live load, as distributed and point loads where appropriate; lumped masses representing the seismic weight are also applied to nodes at member ends. Following ASCE/SEI 41-17 provisions, we apply 5% modal or Rayleigh damping to the linear simulation models unless lower damping levels are justified by experimental testing or other data (e.g., 3% damping was used for the UC Berkeley test frame model). The structures are treated as fully fixed at the base of columns and walls. We include accidental torsion (5% mass eccentricity) if its inclusion increases the torsional amplification factor, η, by more than 10% (ASCE/SEI 41-17 7.2.3.2.2). All deformations and forces from the LDP, including all data presented in this paper, are modified by the linear modification factors, C_1 and C_2, and all deformations and forces caused by accidental torsion are modified by the torsional amplification factor, A_x, (ASCE 41-17 Section 7.4.1.3).

GROUND MOTION

We define the seismic loading using the best estimate of the damaging ground motion recorded either at the base of the structure or nearby the structure's site, described in more

detail in Cook et al. (2023). In the response history LDP, we apply the recorded ground motion directly to the base of the model. For the response spectrum LDP, we use a smoothed demand spectrum from the recorded ground motion. The smoothed demand spectrum reduces noise across close period ranges as is appropriate for input to the response spectrum analysis. To create the smoothed spectra, we calculate spectra from the measured, best-estimate motions for damping ratios between 2% to 20%. Then, we scale each of these spectra to an equivalent spectrum at the target damping (generally 5%) using the B_1 factor per ASCE/SEI 41-17 Section 2.4.1.7.1. The smoothed demand spectrum is taken as the average of the modified spectra, as illustrated in Figure 1(a) for the UC Berkeley test frame for 3% damping (consistent with the modeling approach described above). Figure 1(b) isolates the modified 3% and average 3% spectra, which shows the smoothing effect of the procedure. For the Linear Static method, the spectral acceleration, S_a, is the average modified spectral ordinate at the target damping at the first fundamental period. The effects of kinematic soil-structure interaction on the response spectra are not considered in this study.

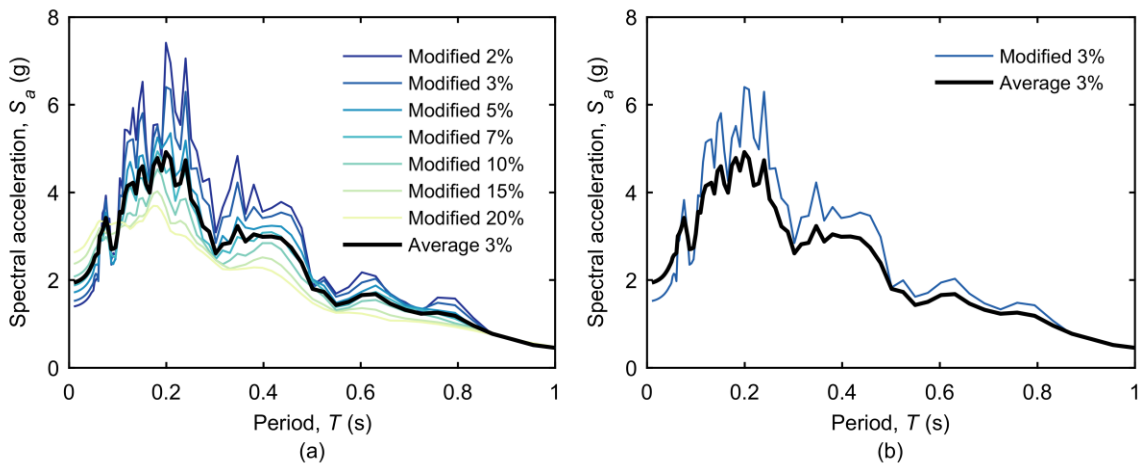

Figure 1. Illustration of determination of smoothed 3%-damping spectrum for linear static and response spectrum assessments for the UC Berkeley test frame motion shown with (a) all modified spectra and (b) 3%-damping spectra only; spectra corresponding to different damping ratios that have been modified by B_1 are used in the smoothing procedure and shown here.

All comparisons in this study, whether qualitative or quantitative, are made without the consideration of uncertainties in either simulated or observed results. ASCE/SEI 41 follows a deterministic approach and, in most cases, does not require the analyst to consider material and modeling uncertainties in the assessment process. Since the goal of this study is to compare simulated outcomes following ASCE/SEI 41 guidelines against recorded building performance, we do not explicitly consider uncertainty in material properties, element stiffness,

or damping. We also do not consider uncertainties in observed damage, recorded response, or ground motion (in cases where recorded ground motions are not available). See Cook et al. (2023) for more discussion on the omission of uncertainties in this study.

COMPARISON OF LINEAR PROCEDURES WITH DAMAGE OBSERVATIONS AND NONLINEAR DYNAMIC PROCEDURES

To benchmark ASCE/SEI 41-17 linear procedures, we compare the outcomes of these procedures to observations of damage and the ASCE/SEI 41-17 NDP outcomes (Cook et al. 2023). In addition, for the buildings where response measurements are available, comparisons are made between the simulated model responses (i.e., drifts and accelerations) and measured responses in the building or specimen. Simulated model responses are directly compared for linear and nonlinear procedures for each model. At the component level, *DCRs* (Eq. 1) targeted at the CP Performance Level are directly compared between linear and nonlinear simulation models; qualitative comparisons are also made between simulated linear *DCRs* and observed damage. Qualitatively, we categorize the observed damage with respect to the descriptions in ASCE/SEI 41, where IO performance implies "only very limited structural damage has occurred" and CP implies "the building is on the verge of partial or total collapse," though it may continue to "support gravity loads." Based on our interpretation of the ASCE/SEI 41 structural performance objective definitions in ASCE/SEI 41-17 Section 2.3.1.5, we judge the observed performance for all buildings in this study, except the Nanhua District Office, as failing the CP acceptance criteria. The assignment of ASCE/SEI 41 acceptance criteria to visible damage is inherently subjective, especially for nonductile components where margins between acceptance criteria are relatively small. This comparison to simulated outcomes may differ if alternative interpretations are justified. Importantly, the ASCE/SEI 41 linear procedures do not underpredict the level of damage in any of our study buildings. Details of the comparisons are described below and summarized in Table 3 at the component level; further information is also available in NIST GCR 22-917-50 (NIST 2022).

Table 3. Summary of the ASCE/SEI 41-17 Linear Procedure component-level evaluations to observed damage and to ASCE/SEI 41 NDP.

Building	Comparison to Observed Damage[a]	Comparison of ASCE/SEI 41 LDP to NDP[b]
UC Berkeley test frame	The evaluation fails CP criteria, which is consistent with observed damage and the physical description of damage associated with CP in ASCE/SEI 41. However, many component simulations exceed CP thresholds that had no observed damage (e.g., joints, beams, and columns at the upper two levels)	More conservative
E-Defense test	The evaluation fails CP criteria, which is consistent with observed damage. However, column and beam component simulations indicate more severe damage than observed due to axial tension caused by wall-frame interaction.	Less conservative[c]
Pyne Gould	The evaluation fails CP criteria, with nearly all frame elements meeting CP and nearly all wall elements exceeding thresholds for CP. The assessment identifies the second-story, transverse direction shear walls as the most critical, which agrees with the most common building mechanism failure theory.	Similar
Imperial County Services	The evaluation fails CP criteria, with all columns at the first story exceeding the CP threshold for both flexure and shear, consistent with observed damage. The assessment also predicts that some columns and beams at upper stories, and some first story walls exceed LS acceptance criteria, and many of the interior joints exceed CP acceptance criteria, despite the limited observed damage.	More conservative
Van Nuys Hotel	The evaluation fails CP criteria, with a significant number of components exceeding the CP threshold. The assessment identifies the highest *DCR* in the third and fourth stories, which is consistent with the location of the highest observed damage; most joint simulations exceed CP at all stories, which is consistent with the frequency and concentration of joint damage observed across the building.	More conservative
Nanhua District Office	The evaluation fails CP criteria, which slightly overestimates the observed damage (judged as beyond LS but within CP). However, the evaluation correctly identifies the direction of most damage (in plan view) as well as the type of failure in the column; the evaluation also identifies some columns as damaged that had no observed damage.	More conservative

[a]Classification of observed acceptance criteria is based on the consensus of the authors.
[b]Judged by comparing (1) the number of components that exceed CP in linear and nonlinear assessments and, for other acceptance criteria, (2) the *DCRs* obtained from the linear and nonlinear model assessments.
[c]In this case, wall CP *DCRs* are lower than *DCRs* in NDP.

BUILDING PERIODS

We calculate the building periods of the six ASCE/SEI 41-17 simulation models according to either eigenvalue or Ritz analysis; calculated building periods are compared to the available measured building periods in Figure 2. The periods of the simulation models, which are based on effective stiffness, are, in general, significantly longer than those measured prior to damaging ground motion. These differences between simulated and measured periods are present even when the values are determined after strong shaking; in this case, the simulated periods are from eigenvalue analysis after the NDP (Cook et al. 2023). ASCE/SEI 41-17

stipulates that all the members in a building should be modeled using stiffness values corresponding to yield levels of cracking. In real buildings, not all members reach yield levels of cracking, particularly at upper stories, and, therefore, the buildings tend to be stiffer than estimated according to those criteria. These differences between measured and simulated periods appear to be greater for RC frame structures (or directions) than RC wall structures (or directions). The wall direction of the Imperial County Services model has a shorter simulated period compared to the measured building period. The real building had significant soil-structure interaction affecting response in the north-south (wall) direction (Kojic et al. 1993), which is not considered in the linear model. The E-Defense building, with periods measured after shaking, also has an underestimated simulated period, but the observed significant wall sliding is not captured by the model.

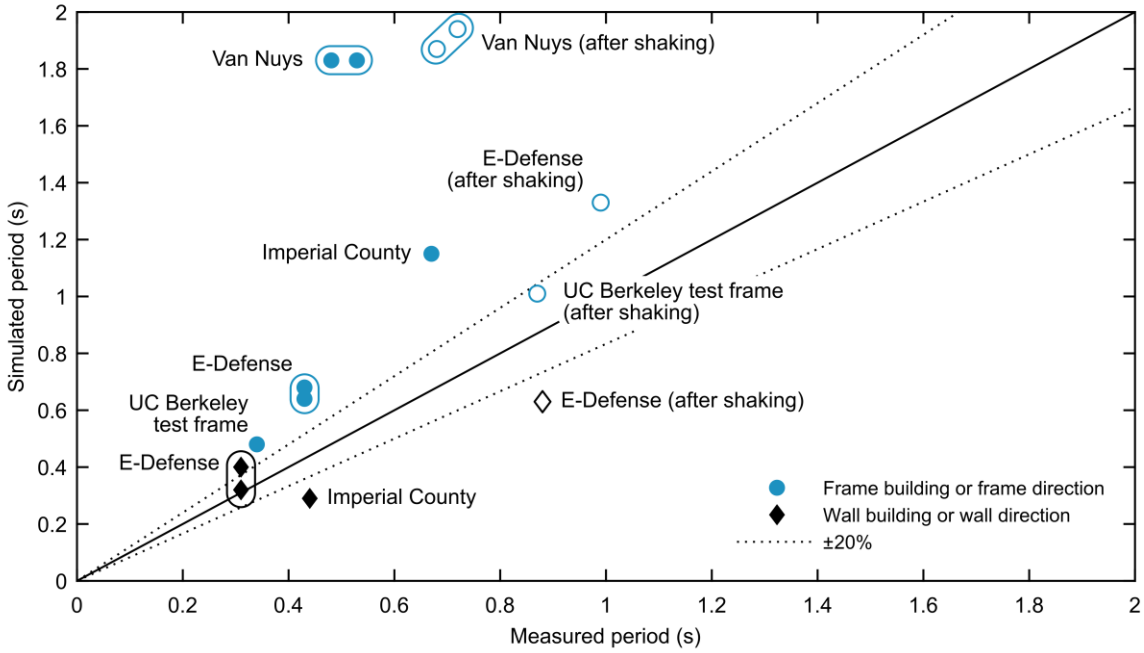

Figure 2. Building fundamental periods: simulated vs. measured. Results are plotted separately for each building direction. Open symbols indicate comparison is made between after-shaking estimates from both simulations and building.

DRIFT DEMANDS AND IDENTIFICATION OF CRITICAL STORY

In the ASCE/SEI 41 linear procedures, drift demands are not directly used as acceptance criteria, but they are proportional to forces and moments developed in the members that are used (in conjunction with *m*-factors) to evaluate performance. For the buildings and models assessed in this study, the ASCE/SEI 41 linear simulations tend to underpredict drifts, sometimes significantly, at the critical locations, as shown in Figure 3(a). The critical locations

are identified by the location of most observed damage in the real structure. The drifts at the critical locations from the linear simulations are also lower than those of the corresponding nonlinear models, as shown in Figure 3(b) with the exception of the E-Defense models in the frame direction. Drifts at other (non-critical) locations are sometimes overpredicted and sometimes underpredicted. For example, the linear simulations of the UC Berkeley test frame underestimate the measured drifts by a relatively modest 10% to 30% at lower stories but overestimate them by about 25% to 90% at the upper stories, depending on the linear procedure used (see Figure 4). For the E-Defense test, the drifts simulated in the shear wall direction differ by roughly 50% from those in the recorded drift response; in the moment frame direction, simulated drifts show better agreement with the recorded drift, though these still overestimate drifts in the upper stories and underestimate drifts in the first story. The instrumented Imperial County Services building provides a comparison of the response history of displacement demands in Figure 5. These results show that there is relatively good agreement between the linear model and the measured response until about 8 seconds into the ground shaking; after this point, significant damage occurred in the building, and the linear simulation model is not able to capture this response. The trend toward underestimation of drifts at critical locations is likely due to the substantial damage and nonlinear response that was incurred in these structures, which cannot be captured by the linear model even with the adjustment factors. These findings are consistent with those of a recent study conducted as part of the ATC 145 project, where the ASCE/SEI 41 LDP was similarly applied to a building that sustained significant damage (ATC 2021).

Due to the inability of linear methods to capture deterioration and damage concentration, the linear simulation models exhibit mixed success in correctly capturing the distribution of drifts over the height of the building. Considering the UC Berkeley test frame (Figure 4), the linear simulations underestimate drifts at the lower story, while overestimating drifts at the upper stories and misidentifying the story of maximum drift. Note that the nonlinear simulation results are discrepant by similar magnitudes but reversed in direction: drifts are overestimated at the lower story and underestimated at upper stories. However, the nonlinear simulation correctly identifies the story with the highest drift demand. In the moment frame direction of the E-Defense test, the models also did not capture the story at which the largest drifts were measured. However, for the Van Nuys building, the observed damage was most severe in the fourth story, consistent with the simulation of peak drifts in the third and fourth

stories of the linear model. For the Nanhua District Office (simulated drift data are unavailable and not shown) and Pyne Gould building models, the linear simulations correctly identified the direction of the maximum response (in plan view) in relation to the observed damage and captured torsional effects.

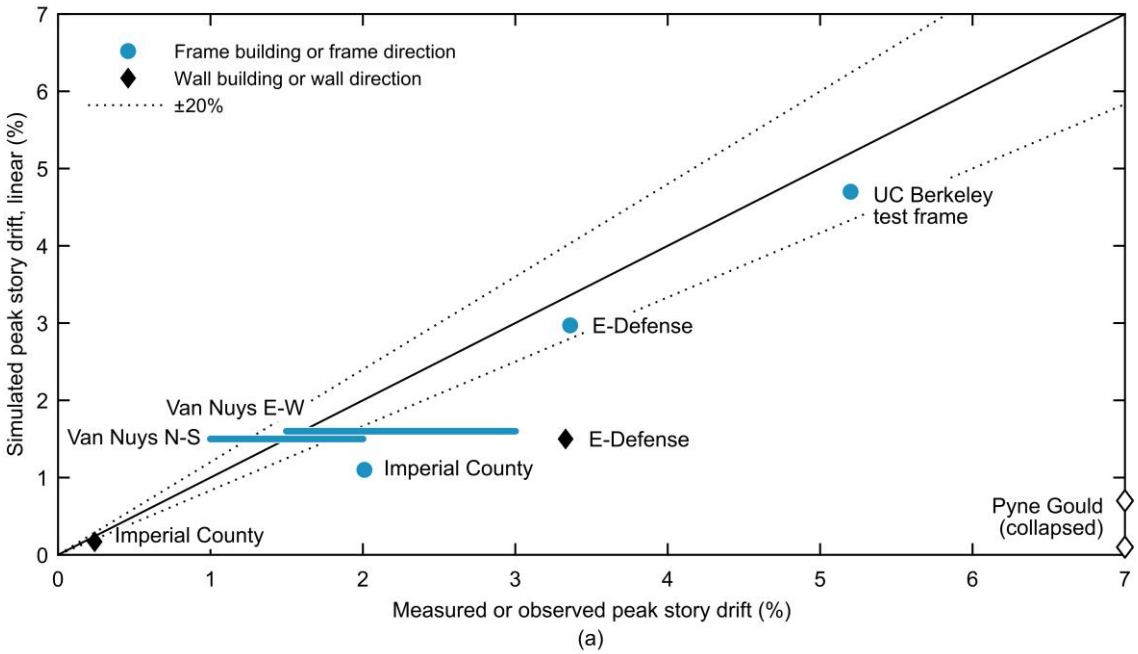

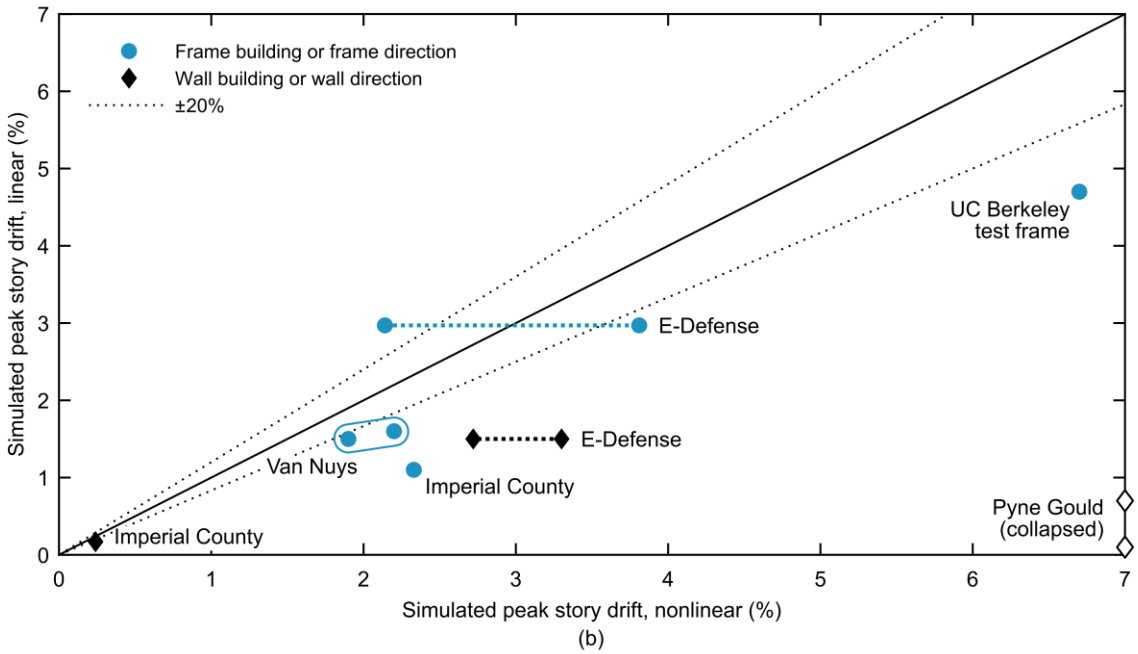

Figure 3. Peak story drifts at critical story (defined by location of largest observed damage): (a) simulated by ASCE/SEI 41-17 LDP vs. measured and (b) simulated by ASCE/SEI 41-17 LDP vs. by ASCE/SEI 41-17 NDP. Results are plotted separately for each building direction. For the E-Defense building, the two nonlinear models (OpenSees and Perform3D) produced different outcomes as shown

in (b). In the Van Nuys building, drifts at the critical location are estimated from measurements at other locations, so a range is provided for the measured outcome in (a).

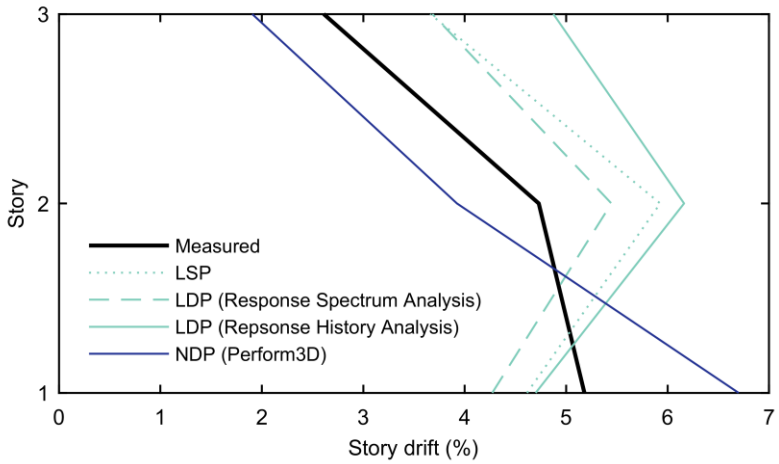

Figure 4. UC Berkeley test frame story drift profiles: simulated by ASCE/SEI 41-17 linear and nonlinear procedures versus measured.

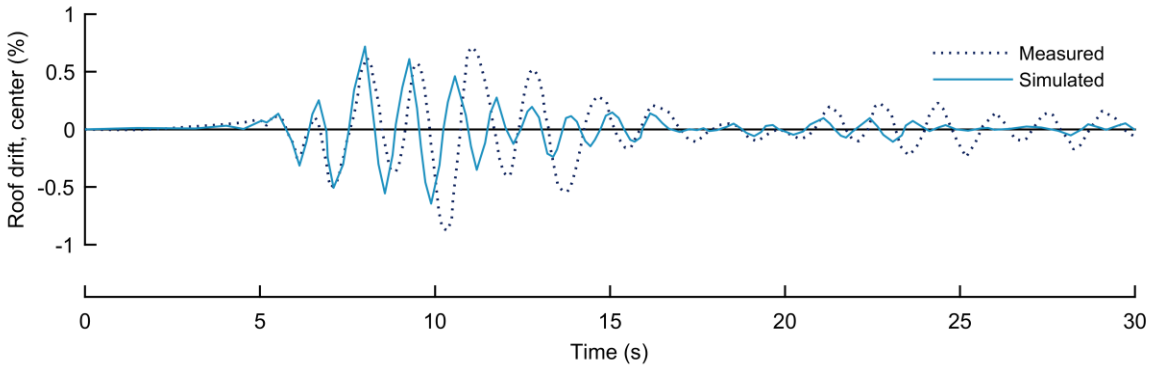

Figure 5. Imperial County Services building roof displacement time history in the frame direction: simulated by ASCE/SEI 41-17 LDP vs. measured.

PEAK ROOF ACCELERATIONS

The simulated peak roof accelerations from the ASCE/SEI 41 linear models show poor agreement with measured response for most buildings, as shown in Figure 6(a), consistently overpredicting acceleration demands. Similarly, the linear models predict higher roof accelerations compared to the results of the ASCE/SEI 41-17 NDP in Figure 6(b), which generally provided good agreement with measured roof accelerations (Cook et al. 2023). We attribute the overestimation of accelerations to the inability of the linear methods to account for yielding of the structure and concentration of response and damage. Overestimating accelerations leads to overestimation of force demands in force-controlled components, including axial loads in columns. We observe similar trends with floor accelerations (not

shown), which suggest demands on nonstructural components computed by Section 13.4.3.1 of ASCE/SEI 41-17 may also be overestimated by the LDP and, by extension, Section 13.3.1.4 of ASCE/SEI 7-16. Note that the floor accelerations estimated by the NDP for the same buildings tend to be overpredicted for frame systems and underpredicted for wall systems, but they more closely match measured values (see Cook et al. [2023]).

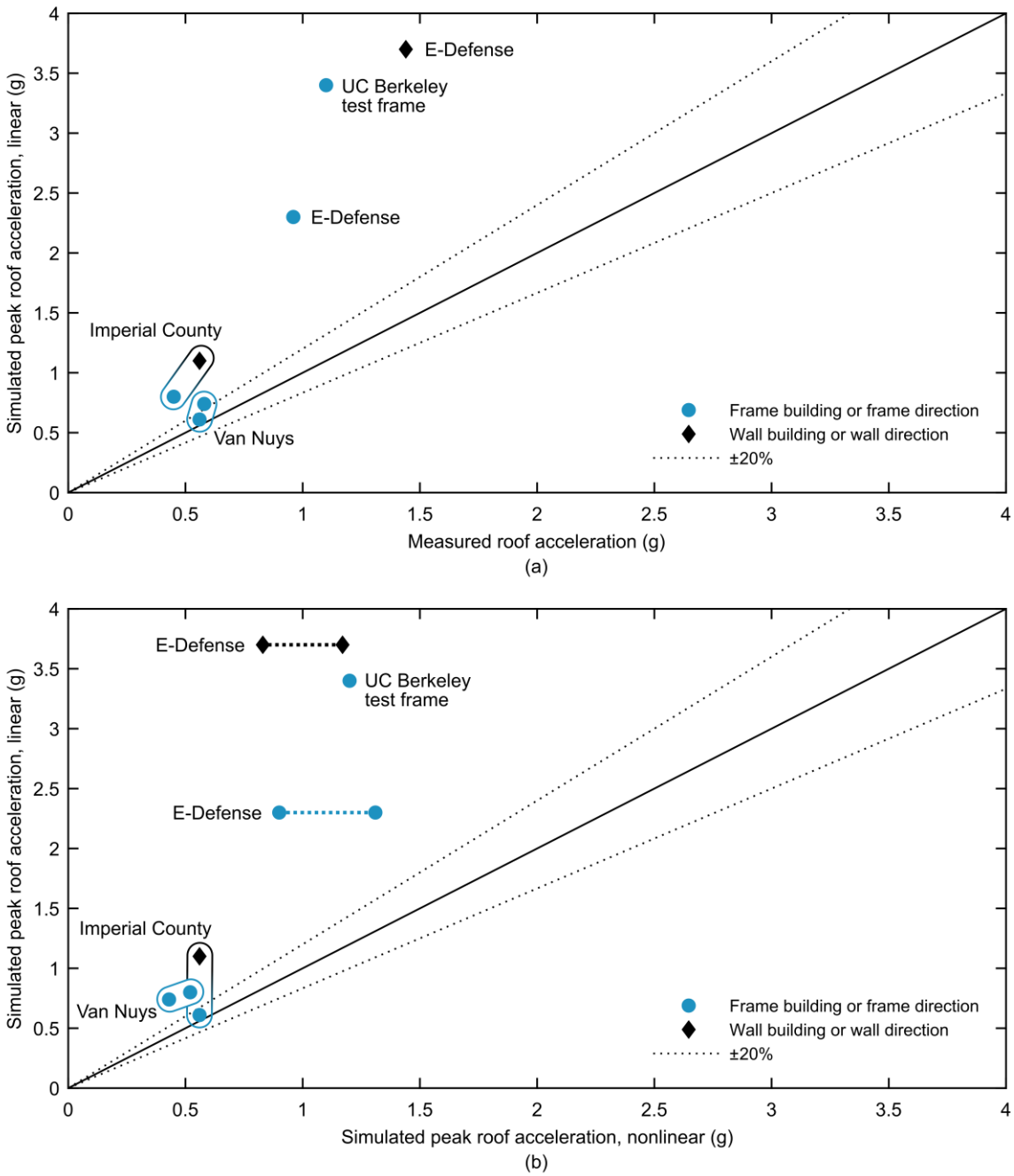

Figure 6. Roof accelerations: (a) simulated by ASCE/SEI 41-17 LDP vs. measured and (b) simulated by ASCE/SEI 41-17 LDP vs. by ASCE/SEI 41-17 NDP. Results are plotted separately for each building direction.

COMPONENT DEMAND-CAPACITY RATIOS AND ACCEPTANCE CRITERIA

To benchmark the component-level assessments from the ASCE/SEI 41-17 linear procedures, we compare component *DCRs* from linear simulations to the observed damage and the component-level assessment from the nonlinear procedures, as summarized in Table 3 and described in more detail here. In all cases, the ASCE/SEI 41-17 linear evaluation finds the building to fail the CP limit state, which is consistent with the observed damage except in the case of the Nanhua District Office building. However, as described in detail below, most models result in a greater number of components identified as exceeding the CP threshold than were observed to be severely damaged, as summarized in Table 3. To the extent that these values are meaningful in a building that is severely damaged, the magnitude of the *DCRs*, meaning the CP threshold was exceeded by a larger margin, were also generally larger in the linear procedures. We note that this conservatism occurs even though drift demands—which are not directly used to evaluate performance but are related to component demands—are, in many cases, underestimated.

Figure 7 illustrates the CP *DCR* results of the ASCE/SEI 41-17 LDP assessment of the Nanhua District Office building. In the North-South direction, none of the components have *DCR* > 1, which is consistent with the observed damage. In the East-West direction, the (deformation-controlled) flexural *DCR* exceeds 1, meaning CP is failed in most of the damaged columns (see also Table 3), which is consistent with the photographs showing spalling indicative of flexural damage. Likewise, most of the columns that sustained damage in the form of diagonal cracking had (deformation-controlled) shear CP *DCR* values that exceeded 1. Thus, we conclude that the model correctly predicts the columns' flexure-shear failure mode. However, the LDP assessment identifies several columns as damaged that were not observed to be damaged after the earthquake and identifies one column as not exceeding the CP threshold that did indeed sustain severe damage (see light green highlighted columns in Figure 7). We also observe that a model neglecting the presence of masonry infill (i.e., noncompliant with ASCE/SEI 41-17) does not correctly predict column failure modes, as expected since the captive column effect is not simulated. While the global damage pattern is similar to the infill models (including no significant torsional effects), the columns in this model have consistently lower CP *DCR* values that suggest a purely flexural failure mode.

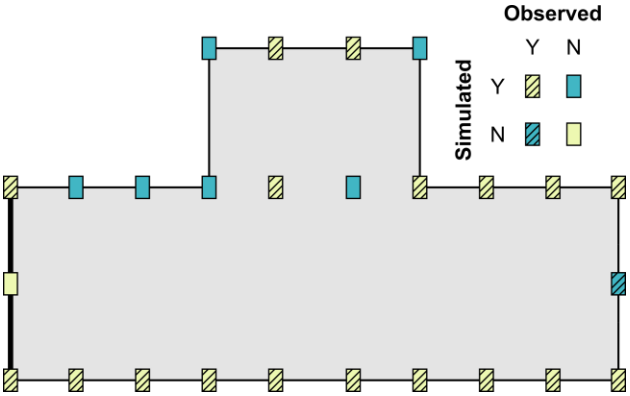

Figure 7. For the Nanhua Building, comparison of simulated vs. observed damage based on flexure and shear CP DCR from linear LDP (response history analysis) in the East-West direction, where Y indicates the component exceeds the CP threshold and the colors indicate whether the observations and simulations agree.

Figure 8 summarizes similar conclusions for the UC Berkeley test frame, where the linear procedures overpredict damage in beams, columns, and joints at upper stories (response history analysis results are shown but deformation demands in other linear procedures are similar, as indicated in Figure 4). In the experiment, damage was concentrated in first-story columns, and column failure precipitated damage to joints (Ghannoum and Moehle 2012). However, the assessment of this structure also illustrates how the linear procedures could be improved by consideration of possible limit state mechanisms. This point is explored by comparing Figure 8(a) and (b). In Figure 8(a), all component demands are taken directly from the LDP (response history analysis), following ASCE/SEI 41's current procedures. However, in Figure 8(b), the beam and joint demands are limited based on yielding of the adjoining column elements (i.e., determined by a mechanism analysis), while the column demands are taken directly from the LDP. Using this approach, the behavior of the beam and joint elements shows much closer agreement to the observed performance. However, the performance of the column elements at the upper two levels still indicates more severe damage than the observed performance even after accounting for the limit state mechanism.

COMPARISON AMONG ASCE/SEI 41-17 LINEAR PROCEDURES

For several of the buildings, the simulations provide a comparison among the different ASCE/SEI 41-17 linear procedures. The different linear procedures applied to the UC Berkeley test frame produce drift demands that are up to 25% different, although they develop similar displaced shapes, as shown in Figure 4. These differences are attributed, in part, to use of the smoothed spectrum in the response spectrum analysis. None of the displaced shapes from the

linear analyses agree well with the measured responses. Acceleration demands computed from the response spectrum procedure using the complete quadratic combination (CQC) method with 9 Ritz modes are also up to 25% different from the response history analysis, but all greatly exceed the measured values. Like the UC Berkeley test frame, the linear response history analysis of the Pyne Gould building results in higher drifts compared to the response spectrum method. However, these drifts are not significantly different and both methods produce a similar distribution of drifts over the height of the building, such that the outcome of the assessment is not sensitive to the linear procedure selection. Taken together, for these highly damaged buildings, in no case does the selection of LDP method (i.e., response spectrum or response history analysis) affect the outcomes of the study, and all LDP results have similar trends in comparison to the observed damage and the NDP. However, the selection of linear procedure may be more important for a less damaged building, and the linear static procedure likely differs substantially from other methods for taller buildings (note that we only examine the static procedure for the two-story UC Berkeley test frame).

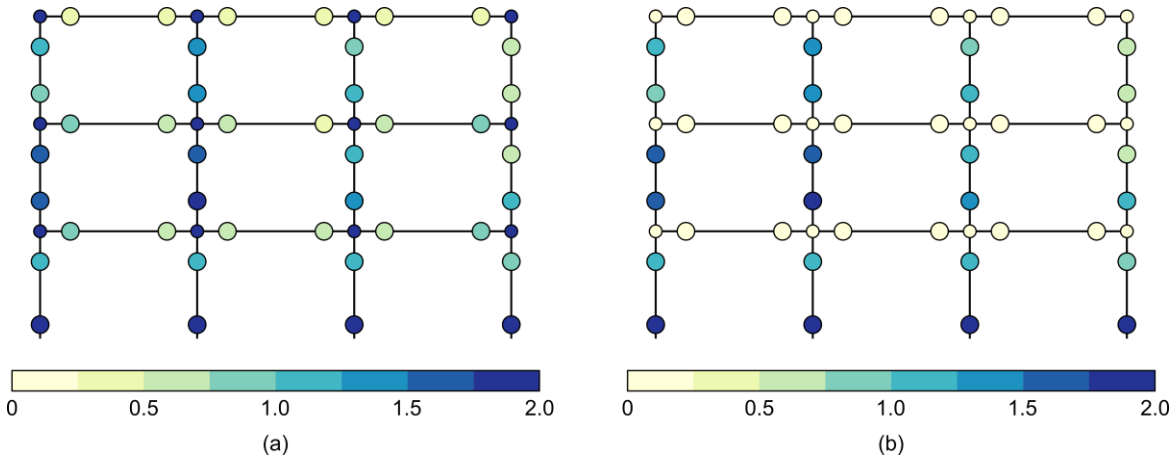

Figure 8. For the UC Berkeley test frame, CP DCR from ASCE/SEI 41-17 (a) LDP response history analysis, with (b) LDP results modified to consider limit state mechanisms in determining force demands on beams and joints.

FEMA P-2018 SEISMIC EVALUATION OF OLDER CONCRETE BUILDINGS FOR COLLAPSE POTENTIAL

FEMA P-2018, *Seismic Evaluation of Older Concrete Buildings for Collapse Potential*, is a new, systematic method for determining the seismic vulnerability of older RC buildings (FEMA 2018; Liel et al. 2020; Holmes et al. 2017). Older concrete buildings are prevalent in the existing building stock, and FEMA P-2018 was developed to facilitate the efficient identification of older concrete buildings that have a high risk of earthquake-induced collapse;

importantly, the assessment is accomplished without testing or nonlinear analyses. The outcome of FEMA P-2018 is a Building Rating between 0.1 and 0.9 representing collapse risk (i.e., an approximate probability of collapse in the ground motion evaluated), with higher Building Ratings indicating greater vulnerability to earthquake-induced collapse; in Chapter 10 of FEMA P-2018, buildings with a Building Rating greater than or equal to 0.7 are classified as exceptionally high risk, between 0.3 and 0.7 as high seismic risk, and less than or equal to 0.3 as lower seismic risk buildings. Here, the FEMA P-2018 Building Ratings are compared to both the observed damage and the CP performance results from the ASCE/SEI 41-17 NDP. We also explore how the mechanism-based (limit-state) collapse analysis in FEMA P-2018 could be used to advance ASCE/SEI 41 linear procedures. The buildings we evaluate through FEMA P-2018 are listed in Table 1.

METHODS

FEMA P-2018 does not require a nonlinear model and, instead, relies on mechanism analysis, analytical drift relations, and structural reliability theory to determine whether a building is collapse prone. The FEMA P-2018 evaluation procedures proceed as follows. First, the building is classified as a frame, frame-wall, bearing wall, or infilled frame system. Subsequently, the building's effective yield strength is determined based on a plastic mechanism analysis and specified procedures for calculating component strengths. Equations are provided for estimating the effective fundamental period, which is intended to represent the effective period of the building in the highly nonlinear (near collapse) regime. A global demand-to-capacity ratio is calculated based on the ratio of seismic demand to capacity, which is referred to as the Global DCR or μ_{strength} (FEMA P-2018 Section 5.7). Presuming that these calculations do not immediately reveal a building is exceptionally high risk (e.g., very weak) or lower risk (e.g., very strong), the subsequent calculations determine global, story, and component drift demands through simplified methods. The global drift demand is a function of the estimated fundamental period (FEMA P-2018 Sections 6.4, 7.4, 8.4, and 9.4). For each component, a Component Rating is determined based on a ratio of component drift demands to capacities. These Component Ratings are combined to determine a Story Rating and finally a Building Rating (maximum Story Rating in either direction), which represents the likelihood of building collapse. We conduct this assessment using the response spectrum developed from the best-estimate ground motion; in the case of the UC Berkeley test frame, the smoothed spectrum is used (refer to Figure 1 and surrounding discussion).

The resulting Building Ratings are compared to the observed performance. For comparison with the FEMA P-2018 rating, we also refer to the collapse fragility curve for each building using the same models developed through the ASCE/SEI 41 NDP (Cook et al. 2023). The collapse fragility curves are developed using an incremental dynamic analysis of the ASCE/SEI 41 nonlinear models. This assessment uses the FEMA P-695 far-field ground motions scaled as a set normalized by peak ground velocity (FEMA 2009). Based on discussions by the ASCE/SEI 41-17 update committee (see Cook and Liel [2021] for more details), we use a story drift of 6% to indicate collapse. Although collapse mechanisms of nonductile RC buildings can be complicated, many of the phenomena, including shear and axial failure, are represented directly by rotational hinge backbone curves that produce (in the simulation models) a sidesway mechanism that can be identified by these drift limits. In addition, intermediate outputs from the FEMA P-2018 methodology, such as building strength, fundamental periods, and critical story and direction are compared to the ASCE/SEI 41 NDP results.

Since the FEMA P-2018 uses a deterministic approach to quantify collapse vulnerability, uncertainties in material properties, structural characteristics, and ground motion intensity were not considered. The collapse fragility curves developed using the incremental dynamic analysis directly consider record-to-record ground motion uncertainty.

COMPARISON OF FEMA P-2018 BUILDING RATINGS WITH DAMAGE OBSERVATIONS AND ASCE/SEI 41 OUTCOMES

The results of the FEMA P-2018 seismic evaluation for collapse potential for four of the studied buildings are provided in Table 4. Figure 9 shows the results graphically with collapse fragility curves developed from incremental dynamic analysis. We assume the lognormal standard deviation parameter, β, is 0.6, based on recommendations from FEMA P-695. To aid comparison between buildings in Figure 9, we normalize spectral acceleration at the building fundamental period, $S_a(T_1)$, by that of the best-estimate ground motion. The FEMA P-2018 Building Ratings have been developed only for the best-estimate ground motions and are therefore plotted at normalized $S_a(T_1)$ of 1.0.

Three of the four buildings we assess using FEMA P-2018 fail the CP performance level in the ASCE/SEI 41 nonlinear assessments (the Nanhua District Office building fails the LS performance level; see Cook et al. [2023]). The FEMA P-2018 results indicate that the

Building Ratings range from 0.3 (on the border between Lower Seismic Risk and High Seismic Risk, according to FEMA, 2018) to 0.9 (Exceptionally High Seismic Risk) for the four buildings assessed. The Pyne Gould building and the UC Berkeley test frame have the highest scores. The Pyne Gould building did in fact collapse, and—in the experiment—the UC Berkeley test frame had one column (out of four) that had suffered significant damage and appeared to be at the onset of axial failure and, therefore, close to precipitating collapse of the whole structure (Ghannoum and Moehle 2012). The E-Defense building had among the lowest ratings at 0.35, consistent with the observed damage; the specimen was not judged to be on the verge of collapse (Wallace et al. 2011). As the Nanhua District Office Building had the lowest damage (below the CP threshold by observation and the NDP), it is consistent that it would have a lower rating. However, we judge the Building Rating of 0.3 as lower than expected and note that, while captive column effects due to partial-height masonry are considered in the assessment, the strength and stiffness of the full-height masonry are neglected. Note that this approach deviates from FEMA P-2018, where the effects of full-height masonry should be considered.

Compared to the ASCE/SEI 41 seismic evaluation for CP, the FEMA P-2018 ratings appear to offer more resolution or distinction between the buildings of interest, all of which were severely damaged. In other words, FEMA P-2018 can separate between the somewhat lower collapse risk of the E-Defense building and the high risk of the Pyne Gould building, whereas the ASCE/SEI 41 procedures result in a classification for both as failing CP. The results also provide Building Ratings that generally track—in a relative sense—with the collapse fragilities developed for the buildings at the intensity at which they were evaluated, as illustrated in Figure 9.

Intermediate outputs from FEMA P-2018, as reported in Table 4, are also compared to the ASCE/SEI 41 model results and the observed damage of these buildings. Figure 10 compares the effective period estimated from FEMA P-2018 to that determined from eigenvalue or Ritz analysis from the ASCE/SEI 41-based linear simulation models of the buildings. In general, the FEMA P-2018 effective periods, T_e, are up to 20% longer than the ASCE/SEI 41 simulation model periods (and even longer in some cases, e.g., the Nanhua District Office). This difference is consistent with the intent of the FEMA P-2018 document, which quantifies a secant, effective period to represent collapse response (FEMA 2018). Comparing the peak roof drift demands in Table 4, the longer periods estimated by FEMA P-

2018 correspond to larger drift demands than those of the ASCE/SEI 41-17 LDP for the buildings and ground motions we evaluate. For the UC Berkeley test frame and wall direction of the E-Defense building, these drift demands more closely match the measured peak response.

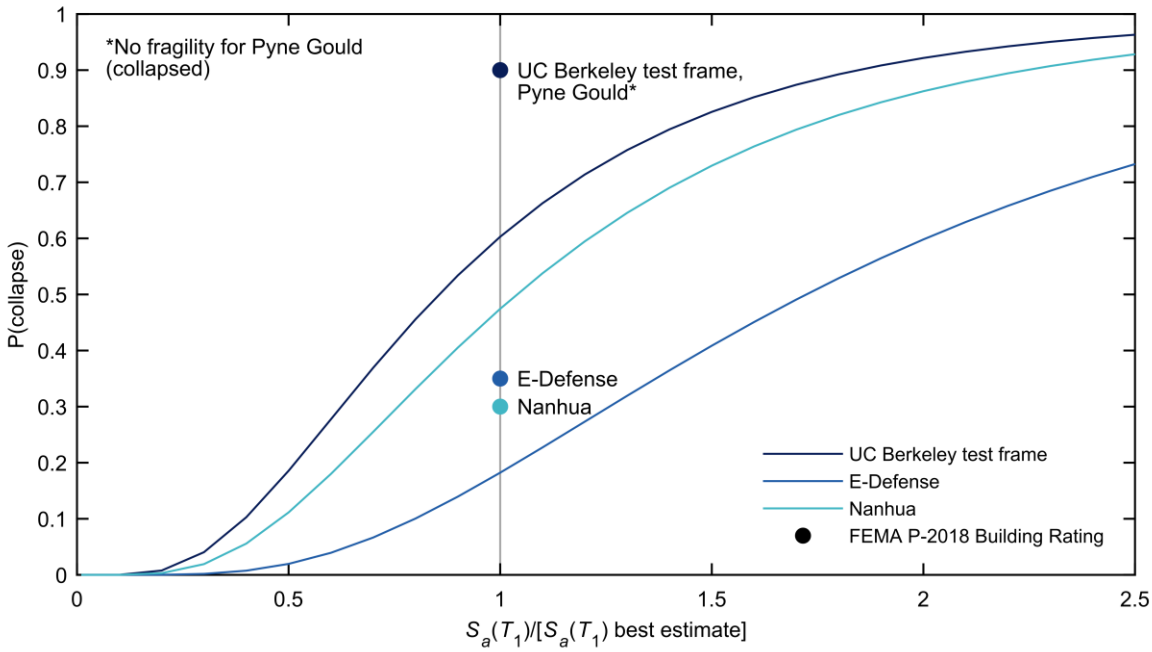

Figure 9. Comparison of FEMA P-2018 ratings (dots) with observed damage and collapse fragility curves. $S_a(T_1)/[S_a(T_1)$ best estimate] is the target spectral acceleration from the collapse fragility assessment normalized by the spectral acceleration used in the FEMA P-2018 assessment, taken as the spectral acceleration at the fundamental period of the building from the recorded ground motion.

In most cases, the FEMA P-2018 evaluation correctly identifies the governing mechanism and the critical story. For example, for the Pyne Gould building, the results of the FEMA P-2018 evaluation are generally consistent with the observed performance of the building; the collapse of this structure is largely attributed to inadequate wall strength in the X-direction, which correlates well with the findings of the P-2018 evaluation in that both the Global DCR, μ_{strength}, and the Building Rating are larger in that direction. Similar observations can be made for the other buildings.

One exception is the FEMA P-2018 evaluation of the E-Defense building, which found some inconsistency in results in the two directions. In the frame-wall direction, a high Global DCR, μ_{strength}, of 6.1 is determined, indicating that the building is weak laterally relative to the demand. This direction also experienced significant, sliding, damage in the walls. However, a Building Rating of 0.10 was calculated in that direction. Although the walls had lost substantial

lateral capacity, FEMA P-2018 is based on tributary gravity loads; because the walls carried relatively low gravity loads, this damage is not reflected significantly in the Building Rating. The Building Rating is assessed to be greater in the other (frame) direction (0.35), which had beam-column joint failure, but not at the same level of damage found in the wall direction. In the frame direction, gravity and lateral loads are shared by the same components. Nevertheless, the overall outcome of 0.35 for the Building Rating is consistent with the observed damage.

Table 4. Summary results of FEMA P-2018 evaluation for the damaged RC buildings

Building	Classification	T_e (s)	Global DCR, $\mu_{strength}$	Governing Mech.[a]	Critical Story	Peak Roof Drift Ratio (%) FEMA P-2018	ASCE 41 LDP	Measured	Story Rating[b]
UC Berkeley test frame	Frame	0.50	4.1	1	1	5.7	4.4	5.4	**0.9**
E-Defense, wall direction	Frame-wall	0.42	6.1	2	1	2.0	1.1	2.7	0.1
E-Defense, frame direction	Frame	0.71	4.4	1	1	2.8	2.1	2.0	**0.35**
Pyne Gould, X-direction	Frame-wall	0.77	23	4	2	2.1	0.5	collapse	**0.9**
Pyne Gould, Y-direction	Frame-wall	0.35	4.4	2	1	0.3	0.1	collapse	0.1
Nanhua, X-direction	Frame	0.88	1.3	2	1	1.7	—	—	0.1
Nanhua, Y-direction	Frame	0.58	1.2	1	1	1.5	—	—	**0.3**

[a]Governing mechanism defined by FEMA P-2018: 1 is first story mechanism, 2 is a distributed beam (complete) mechanism over the height of the building, 4 has a distributed beam mechanism above the story where there is an irregularity (FEMA, 2018).
[b]Building Rating is the maximum Story Rating in either direction; indicated by bold values.

Generally, we conclude that the FEMA P-2018 evaluations provide a reasonable performance evaluation for the four buildings. In particular, they suggest the potential for a FEMA P-2018 evaluation to complement the performance assessment of ASCE/SEI 41 by providing more resolution for the CP performance state. In addition, the FEMA P-2018 procedure, which is based on the plastic mechanism analysis, may provide supplemental information in the cases where the ASCE/SEI 41 linear procedures are used by providing information about locations of damage concentration. The added value of a limit state analysis is shown above in the example of the ASCE/SEI 41 linear analysis for the UC Berkeley test frame in Figure 8.

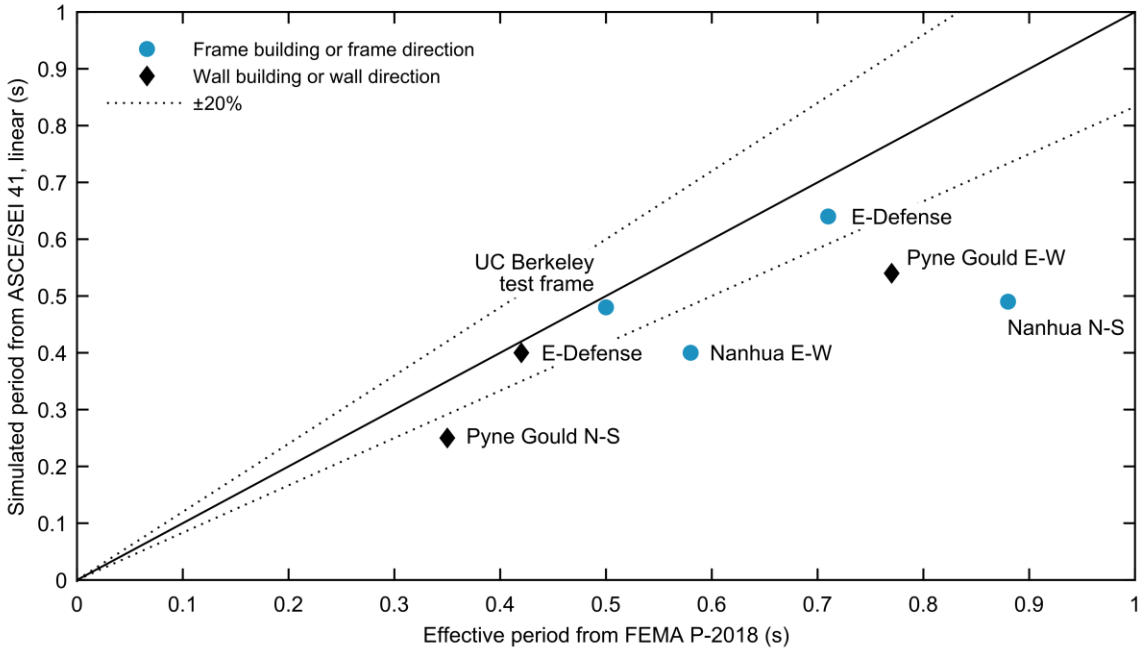

Figure 10. Comparison of effective fundamental period, T_e, from FEMA P-2018 to T_1 from ASCE/SEI 41 linear models.

CONCLUSIONS AND RECOMMENDATIONS

The goal of this study is to examine how well assessments conducted using the linear procedures of ASCE/SEI 41 and the FEMA P-2018 seismic evaluation for collapse potential align with the observed earthquake damage and the ASCE/SEI 41 NDP. To do so, six structures subjected to strong earthquake ground motions are evaluated. Four of the study buildings were real structures shaken by an earthquake and two were experimental specimens tested on shake tables. We use a variety of software packages to create ASCE/SEI 41-17-complaint models and assess performance. To evaluate the outcomes from the various methods, we compare the simulated responses to damage that was measured or observed; comparisons cover global- and component-level response and acceptance criteria. Four of the six structures have detailed recordings and instrumentation from the damaging earthquake motions. In the other two cases, damage descriptions were obtained from photographs and ground motion recordings based on the nearest recording station.

For all buildings, the overall performance level resulting from the ASCE/SEI 41 linear procedures is consistent with the observed damage. In all but one case, the assessment and the observed damage indicate that the buildings fail the CP performance level during the ground motion. In general, the linear procedures also accurately predict the story with the most damage and, in many cases, accurately predict the failure mode of a component (i.e., flexure, shear,

axial, or mixed). However, the linear procedures generally underpredict drifts at the critical location and greatly overpredict accelerations that may be used in performance evaluation of nonstructural components. Considering acceptance criteria, in most cases, we judge the linear procedures to be more conservative than the NDP, either by overpredicting the severity of component damage or the number of components in the CP performance state. Overall, the NDP and LDPs produce similar results for these vulnerable buildings, though nonlinear procedures are capable of identifying specific component damage with greater fidelity. In particular, the linear procedures predict damage in components that would be precluded by yielding or failure of other components in the load path, exaggerating the extent of damage over most of the considered buildings. Results from the different LDPs, i.e., response history and response spectrum methods, and even the LSP (only evaluated for one building), are not significantly different and would not substantially change the outcome of the ASCE/SEI 41-17 assessment for these relatively low-rise and first-mode-dominated buildings. Importantly, the linear assessments predict severe damage in the best-estimate ground motions, even if this damage is judged to be more severe or distributed differently than observed in the real structure. Therefore, in the context of engineering practice, the linear procedures would trigger mitigation efforts and/or use of nonlinear analysis procedures. These findings lead to recommendations for possible improvements for ASCE/SEI 41—particularly the linear procedures that are widely used in engineering practice. Notably, the ASCE/SEI 41 assumptions about component stiffness and the expected level of cracking produce building responses that are overly flexible over the building height. This excess flexibility stems from the fact that some components (e.g., those at higher stories) may sustain less cracking than assumed based on the prescribed effective stiffness; this corresponds to lower peak story drifts than measured in instrumented buildings or predicted by the NDP. We recommend an investigation of the sensitivity of building response to varying stiffness assumptions across the building, including consideration of ductility demand-based effective stiffness as in NZS 3101.1&2:2006 (Standards New Zealand 2006). The study also shows that response for buildings with masonry infill walls, even those with separation between the walls and the frame, cannot be captured without representing the infill in the models. However, our results are not very sensitive to the details of the model for the infill.

The ASCE/SEI 41 linear procedures may be improved with updates to the *m*-factors (or, alternatively, the system-level modification factors, C_1 and C_2), which are critical to those

assessments. However, the fundamental limitation of the linear analysis, in which the seismic load is distributed based on the stiffness but not strength, cannot be overcome through improved *m*-factors, and the redistribution or concentration of the load cannot be identified. This limitation can lead to identifying vulnerabilities that do not exist in the actual structure because their development is prevented by inelastic action elsewhere. This prevention does not imply such vulnerabilities do not benefit from retrofit, but that a system-level understanding of inelastic action is needed to identify and design retrofit solutions. It is recommended that, when using linear models, a supplementary limit-state mechanism analysis such as that defined by FEMA P-2018 evaluation methodology be undertaken to better estimate or bound the demands on components that may be affected by other yielding elements.

This paper also compares the outcome of the FEMA P-2018 simplified collapse evaluation with observed damage and collapse fragilities obtained with an ASCE/SEI 41-compliant nonlinear model. The FEMA P-2018 Building Ratings for collapse potential seem to produce a ranking of collapse vulnerability consistent with observed damage and collapse fragility assessment, with a finer distinction of performance among buildings than provided by the ASCE/SEI 41 CP designation. The FEMA P-2018 evaluations also generally correctly identify the governing mechanism and the critical story. Our study buildings validate the role of FEMA P-2018 as a screening procedure that complements ASCE/SEI 41, where FEMA P-2018 provides a global understanding of seismic vulnerability and ASCE/SEI 41 identifies local (component) vulnerabilities, as needed to inform retrofit.

From a technical perspective, the ASCE/SEI 41 linear procedures and FEMA P-2018 are generally faster and require less expertise to conduct compared to the ASCE/SEI 41 nonlinear procedures—hence, the former is most commonly used in practice. All evaluation procedures require a degree of engineering judgment in both application and interpretation of results, and greater sophistication in analysis approach does not imply greater accuracy. Despite the various shortcomings of the procedures identified, the evaluation methods are reasonably reliable in their ability to predict performance in the heavily damaged structures evaluated in this study, which we judge to be near or beyond CP; it is not clear if this reliability holds for lower levels of damage (i.e., more stringent acceptance criteria).

While the results of this study provide important insights for practicing engineers between expected outcomes from the ASCE/SEI 41 standards, observed building performance and results of other evaluation methods are limited in scope by the lack of consideration of

uncertainties, especially material and modeling uncertainties. Future studies should expand this work to consider modeling and material uncertainties within the bounds of each standard or method assessed here to benchmark the range of results possible, address the potential level of conservatism in overall building performance identified across both linear and nonlinear procedures in ASCE/SEI 41, and, generally, provide additional insight into how future standards could be improved. In addition, while nonstructural component performance is not a focus of this work, future studies may consider system ductility-based adjustments for nonstructural component forces derived from floor accelerations. Finally, the validity and role of FEMA P-2018 in seismic evaluation and retrofit practice should continue to be investigated with a view toward incorporation in relevant standards or codes.

ACKNOWLEDGMENTS

The work forming the basis for this publication was conducted by the Applied Technology Council pursuant to a contract with the National Institute of Standards and Technology under Contract No. SB1341 13 CQ0009/16-476 and 1333ND19PNB730832. The contents of this paper reflect the views of the authors, and do not necessarily reflect the official views or policies of NIST.

Certain commercial software may have been used in the preparation of information contributing to this paper. Identification in this paper is not intended to imply recommendation or endorsement by NIST, nor is it intended to imply that such software is necessarily the best available for the purpose. Also, it is NIST policy to employ the International System of Units (metric units) in all of its publications. However, in the North American construction and building materials industries, certain non-SI units are used, therefore measurement values using both SI and customary units are included in this publication.

REFERENCES

Applied Technology Council (ATC) (2021). *Resilient Repair Guide Source Report: Case Study Annex, ATC 145-2-SRA*, Redwood City, CA.

American Concrete Institute (ACI) (2017). *Standard requirements for seismic evaluation and retrofit of existing concrete buildings, ACI 369.1*, Farmington Hills, MI.

American Society of Civil Engineers (ASCE) (2017). *Seismic evaluation and retrofit of existing buildings, ASCE/SEI 41-17*, Reston, VA.

Computers and Structures, Inc (CSI) (2020). *ETABS*, Software, https://www.csiamerica.com/products/etabs.

CSI (2020). *SAP2000*, Software, https://www.csiamerica.com/products/sap2000.

Cook D, Sen A, Liel A, Basnet T, Creagh A, Koodiani HK, Berkowtiz R, Ghannoum W, Hortacsu A, Kim I, Lehman D, Lowes L, Matamoros A, Naeim F, Sattar S, and Smith R (2023). "ASCE/SEI 41 Assessment of Reinforced Concrete Buildings: Benchmarking Nonlinear Dynamic Procedures with Empirical Damage Observations." *Earthquake Spectra, In Review*.

Cook D and Liel A (2021). "Component Response Metrics for Indication of Global Collapse," *Bulletin of Earthquake Engineering*, https://doi.org/10.1007/s10518-021-01205-x.

Elwood KJ, Matamoros AB, Wallace JW, Lehman DE, Heintz JA, Mitchell AD, Moore MA, Valley MT, Lowes LN, Comartin CD, and Moehle JP (2007). "Update to ASCE/SEI 41 concrete Provisions," *Earthquake Spectra*, 23(3), 493-523.

Elwood KJ and Eberhard MO (2009). "Effective stiffness of reinforced concrete columns," *ACI Structural Journal*, 106(4), 476-84.

Federal Emergency Management Agency (FEMA) (2009). *Quantification of building seismic performance factors, FEMA P-695*, Washington, D.C.

FEMA (2018). *Seismic evaluation of older concrete buildings for collapse potential, FEMA P-2018*, Washington, D.C.

Ghannoum WM and Moehle JP (2012). "Shake-table tests of a concrete frame sustaining column axial failures," *ACI Structural Journal*, 109(3), 393-402.

Ghannoum WM and Matamoros AB (2014). "Nonlinear modeling parameters and acceptance criteria for concrete columns," ACI Special Publication, 297, 1-24.

Harris J and Speicher M (2018). "Assessment of performance-based seismic design methods in ASCE 41 for new steel buildings: Special moment frames," *Earthquake Spectra*, 34(3).

Holmes WT, Liel A, Mehrain M, Moehle J, Somers P, and Heintz J (2017). "Seismic Evaluation of Older Concrete Frame, Frame-wall, and Bearing Wall Buildings for Collapse Potential—ATC 78", *Proceedings of the 2017 SEAOC Convention*.

Kojic S, Trifunac MD, and Anderson JC (1993). "Earthquake response of the Imperial County Services 785 Building in El Centro," *Earthquake Engineering and Engineering Vibration*, 13(4).

Liel AB, Moehle J, Holmes W, Mehrain M, Somers P, and Heintz J (2020). "Seismic Evaluation of Older Concrete Buildings for Collapse Potential," *Proceedings of the 17th World Conference in Earthquake Engineering*, Sendai, Japan.

McKenna F, Fenves GL, Scott MH and Jeremie B (2000). "Open System for Earthquake Engineering Simulation, OpenSEES," Software, http://opensees.berkeley.edu/.

National Institute of Standards and Technology (NIST) (2022). *Benchmarking Evaluation Methodologies for Existing Reinforced Concrete Buildings, NIST GCR 22-917-50*, Gaithersburg, MD.

Sattar S (2018). "Evaluating the consistency between prescriptive and performance-based seismic design approaches for reinforced concrete moment frame buildings" *Engineering Structures*, 174, 919-931.

Sattar S and Hulsey AM (2015). "Assessment of first generation performance-based seismic design methods: Case study of a 4-Story reinforced concrete special moment frame building" *Proceedings of the 2015 ASCE Structures Congress*, Portland, OR.

Structural Engineers Association of Southern California (SEAOSC) (2017). *SEAOSC Design Guide Vol. 1: City of Los Angeles Mandatory Earthquake Hazard Reduction in Existing Non-Ductile Concrete Buildings (NDC)*, International Code Council (ICC), Los Angeles, CA.

Speicher MS and Harris JL (2016a) "Collapse prevention seismic performance assessment of new eccentrically braced frames using ASCE 41," *Engineering Structures*, 117.

Speicher MS and Harris JL (2016b) "Collapse prevention seismic performance assessment of new special concentrically braced frames using ASCE 41," *Engineering Structures*, 126.

Speicher MS and Harris JL (2018) "Collapse prevention seismic performance assessment of new buckling-restrained braced frames using ASCE 41," *Engineering Structures*, 164.

Standards New Zealand (2006). *Concrete structures standard, NZS 3101.1&2:2006*, Wellington, NZ.

Wallace JW, Ghannoum WM, Moehle JP, Sause R, Keller W, Tuna Z, Nagae T, Tahara K, Matsumori T, Shiohara H, Kabeyasawa T, Kono S, and Nishiyama M (2011). *Design and Instrumentation of the 2010 E-Defense Four-Story Reinforced Concrete and Post-Tensioned Concrete Buildings*, *PEER 2011/104*, Berkeley,CA.